Supporting Information

Understanding the Magnetic Anisotropy for Linear Sandwich [Er(COT)]$^+$-based Compounds: A Theoretical Investigation

Man-Man Ding, Tao Shang, Rui Hu and Yi-Quan Zhang*

Jiangsu Key Lab for NSLSCS, School of Physical Science and Technology, Nanjing Normal University, Nanjing 210023, P. R. China.

Table S1. Calculated energy levels (cm^{-1}), $\boldsymbol{g}$ (g_x, g_y, g_z) tensors and predominant m_J values of the lowest eight Kramers doublets (KDs) of complexes **1**−**8** using CASSCF/RASSI-SO with OpenMolcas.[S1]

KDs	**1**			**2**			**3**		
	E	***g***	m_J	*E*	***g***	m_J	*E*	***g***	m_J
1	0.0	0.000 0.000 17.886	±15/2	0.0	0.000 0.000 17.872	±15/2	0.0	0.000 0.000 17.949	±15/2
2	174.0	0.020 0.029 15.453	±13/2	148.8	0.015 0.018 16.333	±13/2	142.4	0.000 0.000 15.540	±13/2
3	223.5	0.657 1.491 12.100	±11/2	201.0	0.608 1.340 14.498	±3/2	271.3	9.615 9.466 1.225	±1/2
4	227.8	0.195 3.271 12.326	±3/2	213.0	0.379 2.069 10.881	±9/2	335.7	0.060 0.089 3.641	±3/2
5	244.4	9.498 5.601 1.065	±5/2	240.6	2.714 3.513 7.655	±1/2	354.7	0.001 0.001 13.104	±11/2
6	254.4	0.173 2.463 11.849	±7/2	250.6	1.935 4.440 7.379	±7/2	431.8	0.036 0.066 6.029	±5/2
7	264.0	7.664 5.791 3.103	±7/2	271.4	0.244 1.147 14.572	±3/2	486.9	0.015 0.022 10.744	±9/2
8	279.9	0.161 0.245 14.448	±9/2	295.6	0.099 0.152 16.069	±11/2	502.6	0.031 0.069 8.416	±7/2
KDs	**4**			**5**			**6**		
	E	***g***	m_J	*E*	***g***	m_J	*E*	***g***	m_J

1	0.0	0.000 0.000 17.933	±15/2	0.0	0.002 0.003 17.808	±15/2	0.0	0.000 0.000 17.947	±15/2
2	164.3	0.062 0.081 15.993	±13/2	158.9	0.316 0.460 15.055	±13/2	175.0	0.007 0.008 15.523	±13/2
3	185.1	0.567 1.956 14.481	±3/2	194.5	0.176 0.990 14.657	±3/2	219.4	10.094 9.007 1.227	±1/2
4	205.3	7.361 5.627 3.447	±1/2	227.9	4.211 5.659 7.221	±1/2	299.3	0.482 0.609 3.652	±3/2
5	222.6	0.655 1.303 9.200	±7/2	248.8	1.347 3.683 7.930	±9/2	402.7	0.008 0.012 13.083	±11/2
6	230.3	0.844 1.434 8.894	±1/2	258.3	0.289 3.685 10.000	±3/2	422.0	0.289 0.432 6.058	±5/2
7	258.5	0.348 0.732 14.970	±5/2	274.0	1.338 2.091 12.607	±7/2	523.4	0.046 0.706 8.545	±7/2
8	275.5	0.484 0.663 15.454	±11/2	300.1	0.174 0.379 15.818	±9/2	530.2	0.330 0.405 10.818	±9/2

KDs	**7**			**8**		
	E	$\boldsymbol{g}$	m_J	E	$\boldsymbol{g}$	m_J
1	0.0	0.000 0.000 17.941	±15/2	0.0	0.000 0.000 17.953	±15/2
2	109.7	3.605 6.187 9.171	±5/2	159.7	0.006 0.006 15.491	±13/2
3	127.4	2.069 5.073 9.248	±7/2	198.4	9.947 9.155 1.242	±1/2
4	140.6	0.042 1.325 8.431	±7/2	272.9	0.357 0.444 3.691	±3/2
5	158.2	7.110 4.592 1.628	±1/2	369.3	0.023 0.025 13.059	±11/2
6	190.4	1.199 1.855 12.118	±1/2	385.7	0.153 0.234 6.083	±5/2

7	203.2	1.282 1.598 11.154	±13/2	476.0	0.059 0.286 11.181	±7/2
8	287.4	0.021 0.040 16.652	±11/2	489.2	0.055 0.161 13.050	±9/2

Table S2. Wave functions with definite projection of the total moment | m_J > for the lowest two or three KDs of complexes **1**–**8**.

	E/cm^{-1}	wave functions
1	0.0	99.2%|±15/2>
	174.0	87.0%|±13/2>+7.9%|±11/2>
	223.5	34.1%|±11/2>+28.3%|±9/2>+20.5%|±7/2>+7.0%|±1/2>+6.6%|±3/2>
2	0.0	98.9%|±15/2>
	148.8	63.8%|±13/2>+26.0%|±11/2>+7.4%|±9/2>
	201.0	32.3%|±3/2>+29.0%|±5/2>+17.0%|±1/2>+11.4%|±7/2>
3	0.0	100%|±15/2>
	142.4	100%|±13/2>
	271.3	99.9|±1/2>
4	0.0	99.7%|±15/2>
	164.3	71.2%|±13/2>+22.1%|±11/2>
5	0.0	98.0%|±15/2>
	158.9	71.6%|±13/2>+14.1%|±11/2>+6.3%|±7/2>
6	0.0	100%|±15/2>
	175.0	99.9|±13/2>
	219.4	99.7|±1/2>
7	0.0	99.9%|±15/2>
	109.7	42.4%|±5/2>+20.3%|±3/2>+19.2%|±7/2>+12.7%|±9/2>
	127.4	26.2%|±7/2>+25.5%|±3/2>+21.0%|±9/2>+15.3%|±5/2>+7.8%|±11/2>
8	0.0	100%|±15/2>
	159.7	99.5%|±13/2>
	198.4	99.1%|±1/2>

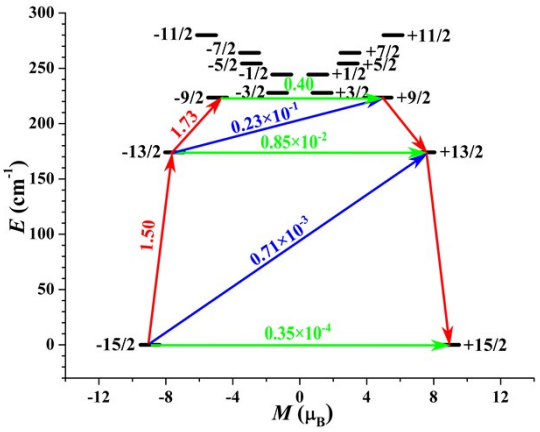
-11/2
-7/2
-5/2
-1/2
-9/2
-3/2
+11/2
+7/2
+5/2
+1/2
+9/2
+3/2
0.40
1.73
0.23×10-1
0.85×10-2
-13/2
+13/2
1.50
0.71×10-3
0.35×10-4
-15/2
+15/2
E (cm-1)
M (μB)

1

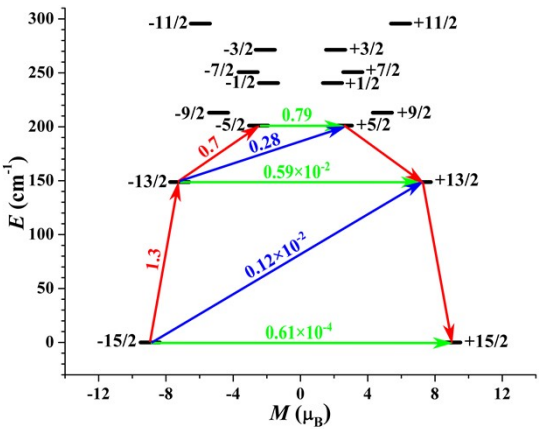
-11/2
+11/2
-3/2
+3/2
-7/2
+7/2
-1/2
+1/2
-9/2
-5/2
0.79
+5/2
+9/2
0.7
0.28
-13/2
0.59×10-2
+13/2
1.3
0.12×10-2
0.61×10-4
-15/2
+15/2
E (cm-1)
M (μB)

2

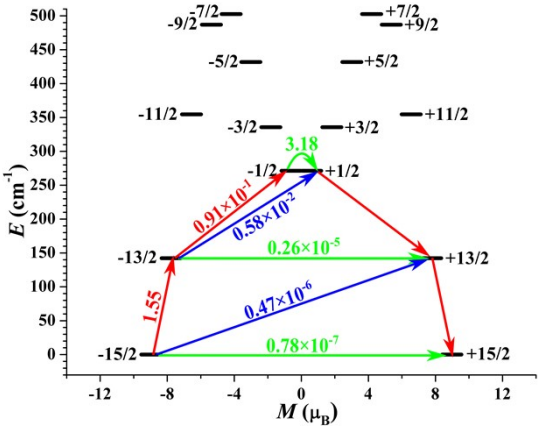
-9/2
-7/2
+7/2
+9/2
-5/2
+5/2
-11/2
-3/2
+3/2
+11/2
3.18
-1/2
+1/2
0.91×10-1
0.58×10-2
0.26×10-5
-13/2
+13/2
1.55
0.47×10-6
0.78×10-7
-15/2
+15/2
E (cm-1)
M (μB)

3

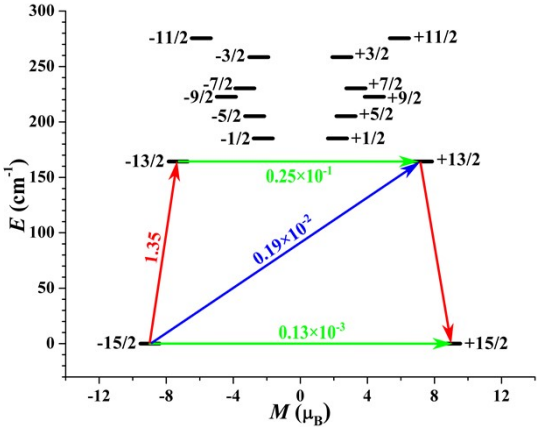
-11/2
+11/2
-3/2
+3/2
-7/2
+7/2
-9/2
+9/2
-5/2
+5/2
-1/2
+1/2
-13/2
0.25×10-1
+13/2
1.35
0.19×10-2
0.13×10-3
-15/2
+15/2
E (cm-1)
M (μB)

4

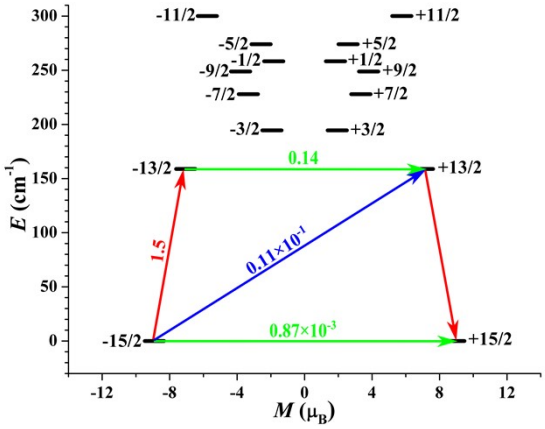
-11/2
+11/2
-5/2
+5/2
-1/2
-9/2
+1/2
+9/2
-7/2
+7/2
-3/2
+3/2
0.14
-13/2
+13/2
1.5
0.11×10-1
0.87×10-3
-15/2
+15/2
E (cm-1)
M (μB)

5

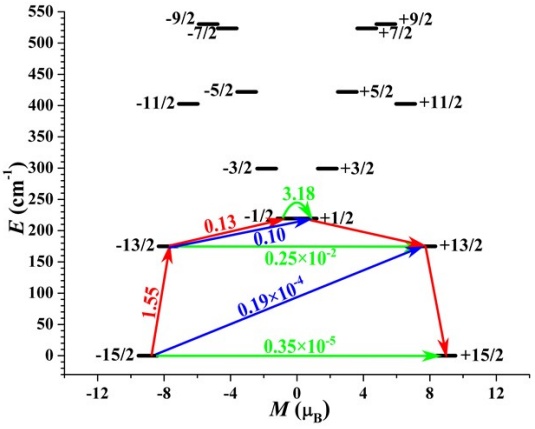
-9/2
-7/2
+9/2
+7/2
-11/2
-5/2
+5/2
+11/2
-3/2
+3/2
3.18
0.13
-1/2
+1/2
0.10
-13/2
+13/2
0.25×10-2
1.55
0.19×10-4
0.35×10-5
-15/2
+15/2
E (cm-1)
M (μB)

6

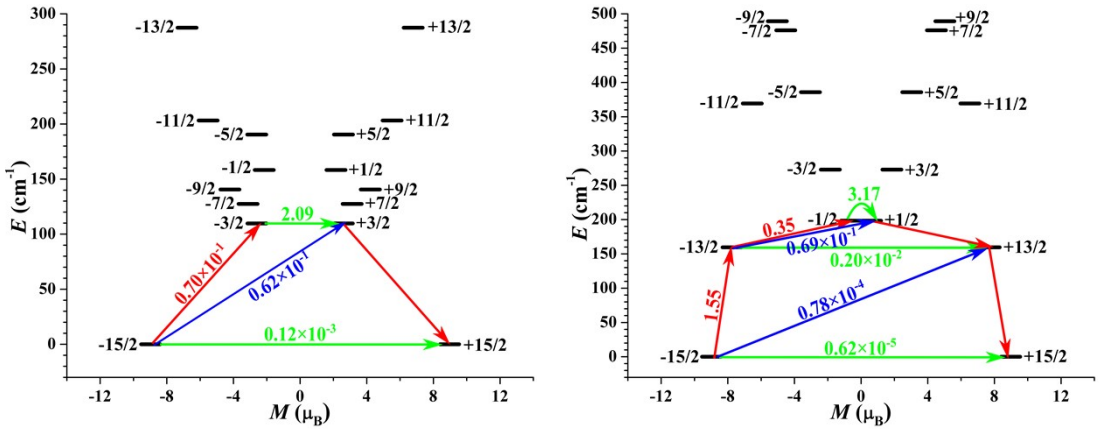

Figure S1. Magnetization blocking barriers in complexes **1**–**8**. The thick black lines represent the KDs as a function of their magnetic moments along the magnetic axes. The green lines correspond to diagonal quantum tunneling of magnetization (QTM); the blue lines represent Orbach relaxation process. The path shown by the red arrows represents the most possibly path for magnetic relaxation in the corresponding compounds. The numbers at each arrow stand for the mean absolute value of the corresponding matrix element of transition magnetic moment.

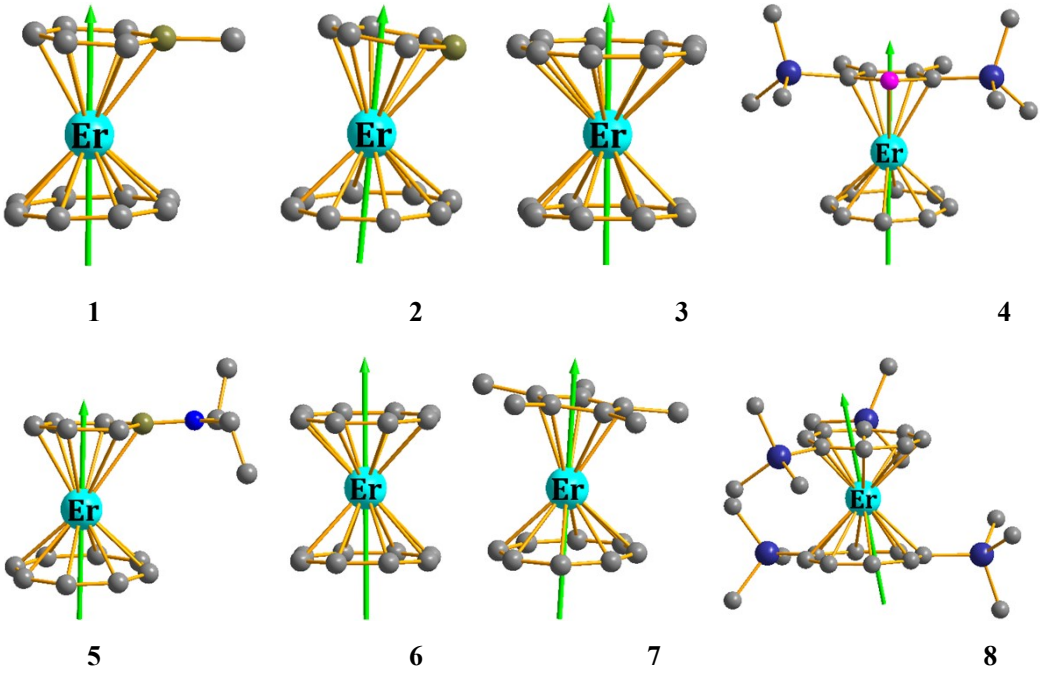

Figure S2. Calculated orientations of the local main magnetic axes on Er^{III} ions of complexes **1**–**8** in the ground KDs.

We have divided the basis sets used in complete-active-space self-consistent field (CASSCF) calculation into three categories: (1) The largest basis (L): ANO-RCC-VQZP for Er^{III} ion; ANO-RCC-VTZP for close C and B atoms; ANO-RCC-VDZ for distant atoms; (2) The medium basis (M): ANO-RCC-VTZP for Er^{III} ion; ANO-RCC-

VTZ for close C and B atoms; ANO-RCC-VDZ for distant atoms; (3) The smallest basis (S): ANO-RCC-VDZP for Er^{III} ion; ANO-RCC-VDZP and VDZ for close C and P atoms, respectively; ANO-RCC-VDZ for distant atoms. Then, ORCA 5.0.1[S2] calculations were performed with CASSCF, followed by N-electron valence second-order perturbation theory (NEVPT2).[S3–S6] SARC2-DKH-QZVP basis set was used for Er^{III},[S7] and DKH-DEF2-TZVP[S8,S9] was for the other atoms. The NEVPT2 calculation with eleven 4*f* electrons in 7 active orbitals (CAS (11, 7)). In the calculations, the orbitals were determined for the average of 35 $S = 3/2$ and 112 $S = 1/2$ roots.

Table S3. Calculated energy levels (cm^{-1}), $\boldsymbol{g}$ (g_x, g_y, g_z) tensors and predominant m_J values of the lowest eight KDs for **6** ($[Er(COT)_2]^-$) with dihedral angle (φ) ranging from 0° to 25° using CASSCF/RASSI-SO with OpenMolcas.

KDs	**0°**			**5°**			**10°**		
	E	***g***	m_J	*E*	***g***	m_J	*E*	***g***	m_J
1	0.0	0.000 0.000 17.947	±15/2	0.0	0.000 0.000 17.946	±15/2	0.0	0.000 0.000 17.943	±15/2
2	175.0	0.007 0.008 15.523	±13/2	171.3	0.015 0.017 15.520	±13/2	160.1	0.071 0.074 15.479	±13/2
3	219.4	10.093 9.008 1.227	±1/2	217.3	9.839 9.249 1.235	±1/2	209.7	10.169 8.780 1.267	±1/2
4	299.3	0.481 0.609 3.652	±3/2	297.7	0.225 0.373 3.672	±3/2	292.1	0.472 0.841 3.697	±3/2
5	402.7	0.008 0.012 13.083	±11/2	399.2	0.004 0.008 13.070	±11/2	389.6	0.006 0.033 13.023	±11/2
6	422.0	0.289 0.432 6.058	±5/2	420.9	0.515 0.665 6.157	±5/2	416.8	1.197 1.576 6.357	±5/2
7	523.4	0.046 0.706 8.547	±7/2	510.7	0.343 0.541 11.482	±7/2	499.7	1.036 1.263 10.490	±7/2
8	530.2	0.330 0.405 10.819	±9/2	547.0	0.066 0.105 14.343	±9/2	567.6	0.139 0.186 15.087	±9/2
KDs	**15°**			**20°**			**25°**		
	E	***g***	m_J	*E*	***g***	m_J	*E*	***g***	m_J

1	0.0	0.002 0.003 17.929	±15/2	0.0	0.024 0.031 17.867	±15/2	0.0	0.067 0.175 16.715	±15/2
2	140.9	0.282 0.301 15.261	±13/2	110.5	1.092 1.444 13.952	±13/2	64.6	3.068 4.240 9.377	±13/2
3	191.5	11.337 6.995 1.367	±1/2	153.3	2.275 4.190 11.496	±1/2	107.9	8.626 5.431 0.930	±11/2
4	279.9	1.429 2.482 3.659	±3/2	256.0	4.565 3.200 1.755	±3/2	225.5	5.374 2.931 0.131	±1/2
5	376.4	0.024 0.165 12.760	±11/2	363.4	0.242 0.633 11.797	±11/2	356.9	0.814 1.920 9.523	±9/2
6	407.7	2.166 3.355 6.306	±5/2	388.3	5.997 5.414 2.900	±5/2	375.4	0.043 0.437 9.059	±13/2
7	491.7	2.292 2.629 9.961	±7/2	487.7	3.243 4.463 9.934	±7/2	509.3	9.885 6.422 2.897	±5/2
8	581.5	0.226 0.292 15.431	±9/2	580.4	0.360 0.440 15.399	±9/2	570.4	0.606 0.869 14.688	±11/2

Table S4. Wave functions with definite projection of the total moment | m_J > for the lowest two or three KDs for 6 with φ ranging from 0° to 25°.

φ	E/cm^{-1}	wave functions
0°	0.0	100%|±15/2>
	175.0	99.9%|±13/2>
	219.4	99.7%|±1/2>
5°	0.0	100%|±15/2>
	171.3	99.6%|±13/2>
	217.3	99.4%|±1/2>
10°	0.0	100%|±15/2>
	160.1	98.7%|±13/2>
	209.7	98.4%|±1/2>
15°	0.0	99.8%|±15/2>
	140.9	96.1%|±13/2>
20°	0.0	99.2%|±15/2>
	110.5	85.5%|±13/2>+7.8%|±1/2>
25°	0.0	86.6%|±15/2>+4.4%|±7/2>
	64.6	31.5%|±13/2>+24.2%|±5/2>+17.1%|±3/2>+12.2%|±11/2>+6.1%|±9/2>

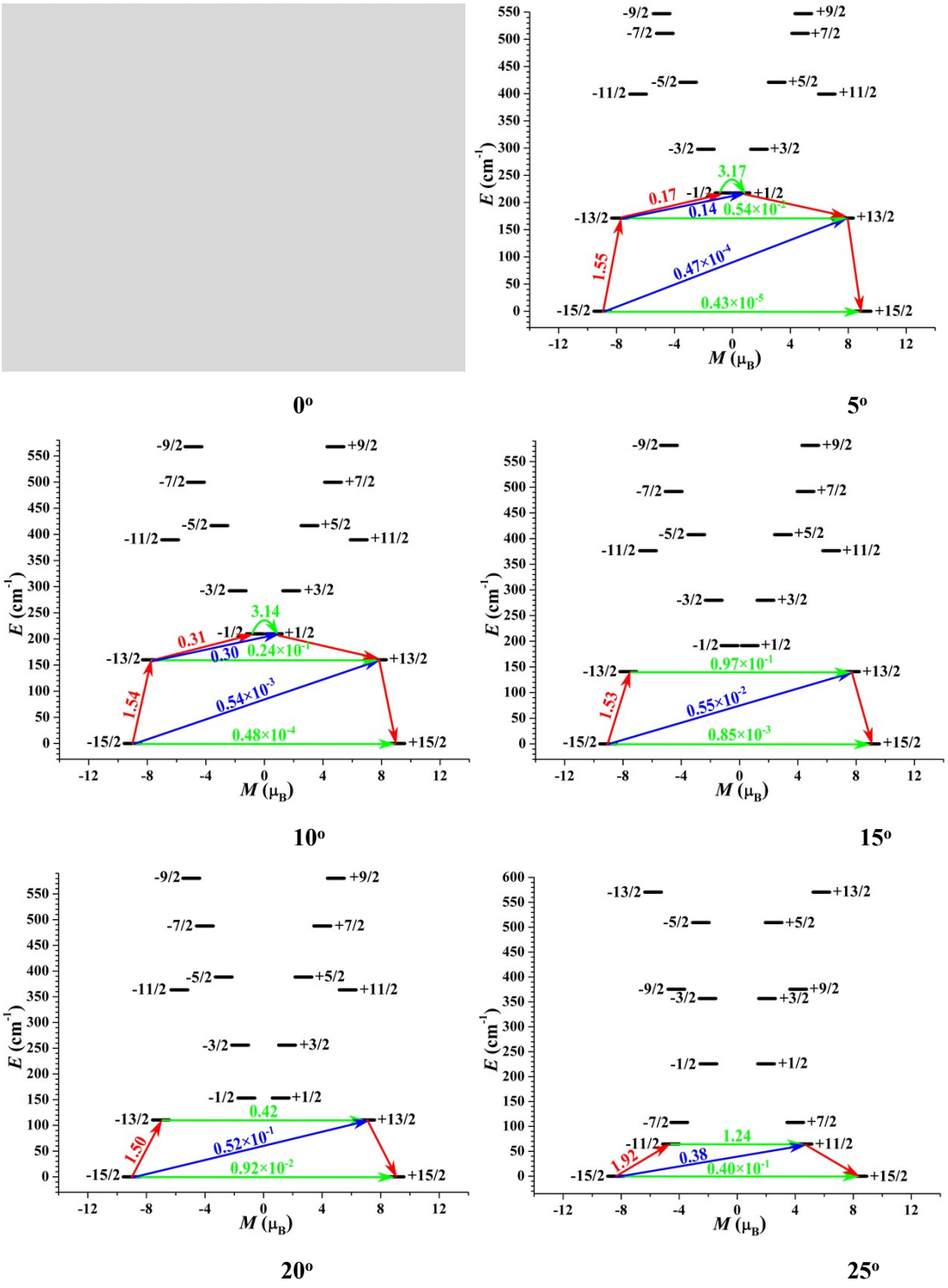

Figure S3. Magnetization blocking barriers for **6** with φ ranging from 0° to 25°. The thick black lines represent the KDs as a function of their magnetic moments along the magnetic axes. The green lines correspond to diagonal quantum tunneling of magnetization (QTM); the blue lines represent Orbach relaxation process. The path shown by the red arrows represents the most possibly path for magnetic relaxation in the corresponding compounds. The numbers at each arrow stand for the mean absolute value of the corresponding matrix element of transition magnetic moment.

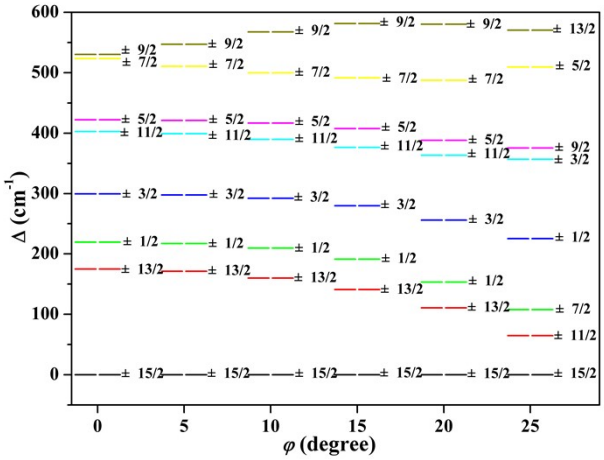

Figure S4. Splitting of the spin-orbit coupled (*J*) ground state by the crystal field for **6**.

Table S5. Calculated crystal-field parameters *B* (*k, q*) and the corresponding weights for **6** with *φ* ranging from 0° to 25°.

0°				**5°**				**10°**			
k	*q*	*B* (*k*, *q*)	weight (%)	*k*	*q*	*B* (*k*, *q*)	Weight (%)	*k*	*q*	*B* (*k*, *q*)	Weight (%)
4	0	-0.12×10^{-1}	38.68	4	0	-0.12×10^{-1}	34.03	4	0	-0.12×10^{-1}	29.26
2	0	-0.17×10^{1}	29.31	2	0	-0.17×10^{1}	25.86	2	0	-0.17×10^{1}	22.26
6	0	0.66×10^{-4}	19.43	6	0	0.67×10^{-4}	17.42	6	0	0.71×10^{-4}	15.81
2	2	0.98×10^{-1}	1.68	2	–1	0.26	3.96	2	–1	0.58	7.61
15°				**20°**				**25°**			
k	*q*	*B* (*k*, *q*)	Weight (%)	*k*	*q*	*B* (*k*, *q*)	Weight (%)	*k*	*q*	*B* (*k*, *q*)	Weight (%)
4	0	-0.12×10^{-1}	25.91	4	0	-0.12×10^{-1}	22.13	4	–1	0.14×10^{-1}	14.52
2	0	-0.17×10^{1}	19.28	2	0	-0.15×10^{1}	15.06	6	–1	-0.14×10^{-3}	14.21
6	0	0.77×10^{-4}	15.14	6	0	0.82×10^{-4}	13.69	4	0	-0.72×10^{-2}	7.69
2	–1	–0.84	9.68	2	–1	–0.91	8.97	2	–1	0.11	6.76

Table S6 Included *θ* (degree) angles for compound **6**.

∠C_1–Er–axis	43.8°	∠C_2–Er–axis	43.9°	∠C_3–Er–axis	44.4°	∠C_4–Er–axis	44.4°
∠C_5–Er–axis	44.3°	∠C_6–Er–axis	44.4°	∠C_7–Er–axis	44.7°	∠C_8–Er–axis	44.4°
∠C_9–Er–axis	44.4°	∠C_{10}–Er–axis	43.8°	∠C_{11}–Er–axis	43.9°	∠C_{12}–Er–axis	44.3°
∠C_{13}–Er–axis	44.4°	∠C_{14}–Er–axis	44.3°	∠C_{15}–Er–axis	44.5°	∠C_{16}–Er–axis	44.7°
∠Average	44.3°						

Table S7. Calculated energy levels (cm^{-1}), ***g*** (g_x, g_y, g_z) tensors and predominant m_J values of the lowest eight KDs for **6** with different included *θ* angle (change the *θ* angles on the one side of COT ligands) keeping the Er-C bond lengths fixed using CASSCF/RASSI-SO with OpenMolcas.

θ / KDs	**36.3°**			**38.3°**			**40.3°**		
	E	***g***	m_J	*E*	***g***	m_J	*E*	***g***	m_J
1	0.0	0.000	±15/2	0.0	0.000	±15/2	0.0	0.000	±15/2

		0.000 17.950			0.000 17.949			0.000 17.949	
2	237.9	5.090 6.165 7.609	±1/2	225.9	0.082 0.094 15.397	±13/2	210.3	0.021 0.023 15.497	±13/2
3	239.6	2.514 2.998 11.293	±13/2	235.0	10.240 8.687 1.334	±1/2	230.6	10.228 8.838 1.243	±1/2
4	303.8	0.796 0.973 3.640	±3/2	303.8	0.710 0.868 3.643	±3/2	303.1	0.627 0.772 3.646	±3/2
5	406.7	0.209 0.401 6.043	±5/2	411.6	0.238 0.408 6.051	±5/2	415.9	0.282 0.431 6.103	±5/2
6	437.1	0.011 0.014 13.078	±11/2	431.3	0.013 0.018 13.078	±11/2	423.5	0.030 0.038 13.027	±11/2
7	499.7	0.226 0.350 8.449	±7/2	506.9	0.216 0.385 8.443	±7/2	513.6	0.192 0.436 8.444	±7/2
8	523.8	0.055 0.064 10.768	±9/2	527.4	0.073 0.088 10.763	±9/2	529.7	0.106 0.129 10.762	±9/2
θ	**42.3°**			**43.3°**			**44.3°**		
KDs	E	$\boldsymbol{g}$	m_J	E	$\boldsymbol{g}$	m_J	E	$\boldsymbol{g}$	m_J
1	0.0	0.000 0.000 17.948	±15/2	0.0	0.000 0.000 17.947	±15/2	0.0	0.000 0.000 17.947	±15/2
2	193.1	0.011 0.012 15.516	±13/2	184.1	0.008 0.009 15.520	±13/2	175.0	0.007 0.008 15.523	±13/2
3	225.4	10.160 8.932 1.230	±1/2	222.5	10.127 8.971 1.228	±1/2	219.4	10.094 9.007 1.227	±1/2
4	301.6	0.549 0.683 3.649	±3/2	300.6	0.515 0.646 3.651	±3/2	299.3	0.482 0.609 3.652	±3/2
5	413.7	0.026 0.047 12.997	±11/2	408.3	0.013 0.020 13.072	±11/2	402.7	0.008 0.012 13.083	±11/2
6	419.6	0.229 0.384 6.131	±5/2	420.9	0.268 0.415 6.067	±5/2	422.0	0.289 0.432 6.058	±5/2
7	519.2	0.131	±7/2	521.5	0.067	±7/2	523.4	0.046	±7/2

		0.521 8.462			0.593 8.487			0.706 8.545	
8	530.7	0.170 0.208 10.770	±9/2	530.6	0.230 0.282 10.784	±9/2	530.2	0.330 0.405 10.818	±9/2
θ / KDs	**45.3°**			**46.3°**			**48.3°**		
	E	g	m_J	E	g	m_J	E	g	m_J
1	0.0	0.000 0.000 17.946	±15/2	0.0	0.000 0.000 17.946	±15/2	0.0	0.000 0.000 17.945	±15/2
2	165.8	0.006 0.007 15.526	±13/2	156.8	0.006 0.006 15.528	±13/2	139.5	0.005 0.005 15.531	±13/2
3	216.4	10.063 9.041 1.227	±1/2	213.3	10.035 9.071 1.227	±1/2	207.2	9.985 9.122 1.227	±1/2
4	297.8	0.451 0.576 3.654	±3/2	296.3	0.423 0.546 3.655	±3/2	292.8	0.373 0.495 3.658	±3/2
5	396.8	0.006 0.009 13.086	±11/2	390.7	0.005 0.007 13.087	±11/2	378.4	0.003 0.005 13.086	±11/2
6	422.7	0.307 0.448 6.057	±5/2	423.1	0.324 0.463 6.057	±5/2	423.0	0.359 0.497 6.058	±5/2
7	524.9	0.277 0.925 8.718	±7/2	525.9	0.767 1.510 9.555	±7/2	524.1	1.033 1.220 11.029	±9/2
8	529.3	0.537 0.648 10.919	±9/2	528.1	1.080 1.228 11.410	±9/2	526.9	0.596 1.512 9.058	±7/2
θ / KDs	**50.3°**			**52.3°**			**54.3°**		
	E	g	m_J	E	g	m_J	E	g	m_J
1	0.0	0.000 0.000 17.944	±15/2	0.0	0.000 0.000 17.943	±15/2	0.0	0.000 0.000 17.942	±15/2
2	123.8	0.005 0.005 15.532	±13/2	110.1	0.005 0.005 15.533	±13/2	99.2	0.005 0.005 15.533	±13/2
3	201.6	9.945 9.162 1.228	±1/2	197.0	9.914 9.192 1.228	±1/2	193.7	9.892 9.212 1.229	±1/2
4	289.2	0.332 0.455	±3/2	285.7	0.301 0.427	±3/2	282.5	0.278 0.409	±3/2

		3.660			3.661			3.662	
5	366.1	0.002 0.005 13.084	±11/2	354.4	0.001 0.005 13.081	±11/2	343.5	0.001 0.006 13.077	±11/2
6	421.7	0.396 0.537 6.060	±5/2	419.3	0.436 0.584 6.061	±5/2	415.9	0.482 0.639 6.062	±5/2
7	519.1	0.490 0.625 10.736	±9/2	512.8	0.363 0.473 10.701	±9/2	505.2	0.318 0.420 10.687	±9/2
8	525.9	0.011 1.066 8.481	±7/2	523.0	0.162 0.966 8.414	±7/2	518.3	0.260 0.964 8.391	±7/2

Table S8. Wave functions with definite projection of the total moment | m_J > for the lowest two or three KDs of **6** with different included θ angle (change the θ angles on the one side of COT ligands) keeping the Er-C bond lengths fixed.

θ	E/cm^{-1}	wave functions
36.3°	0.0	100%|±15/2>
	237.9	70.2%|±1/2>+29.5%|±13/2>
38.3°	0.0	100%|±15/2>
	225.9	99.0%|±13/2>
	235.0	98.8%|±1/2>
40.3°	0.0	100%|±15/2>
	210.3	99.7%|±13/2>
	230.6	99.5%|±1/2>
42.3°	0.0	100%|±15/2>
	193.1	99.8%|±13/2>
	225.4	99.7%|±1/2>
43.3°	0.0	100%|±15/2>
	184.1	99.9%|±13/2>
	222.5	99.7%|±1/2>
44.3°	0.0	100%|±15/2>
	175.0	99.9%|±13/2>
	219.4	99.7%|±1/2>
45.3°	0.0	100%|±15/2>
	165.8	99.9%|±13/2>
	216.4	99.7%|±1/2>
46.3°	0.0	100%|±15/2>
	156.8	99.9%|±13/2>
	213.3	99.7%|±1/2>
48.3°	0.0	100%|±15/2>
	139.5	99.9%|±13/2>

	207.2	99.8%|±1/2>
50.3°	0.0	100%|±15/2>
	123.8	99.9%|±13/2>
	201.6	99.7%|±1/2>
52.3°	0.0	100%|±15/2>
	110.1	99.9%|±13/2>
	197.0	99.7%|±1/2>
54.3°	0.0	100%|±15/2>
	99.2	99.9%|±13/2>
	193.7	99.7%|±1/2>

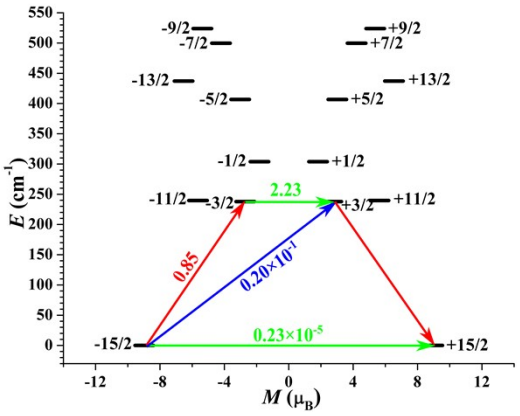

36.3°

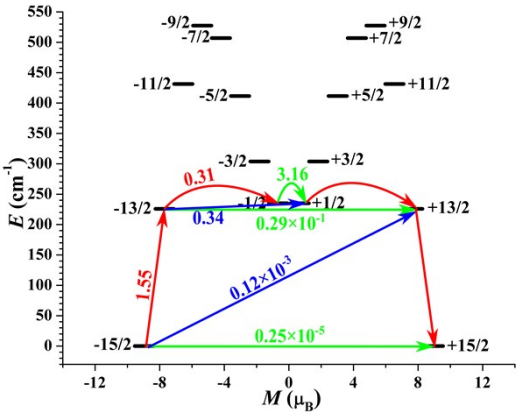

38.3°

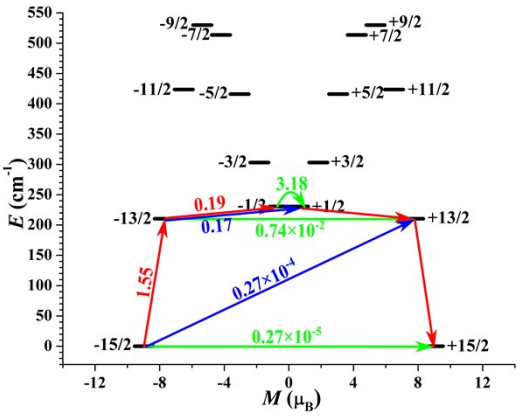

40.3°

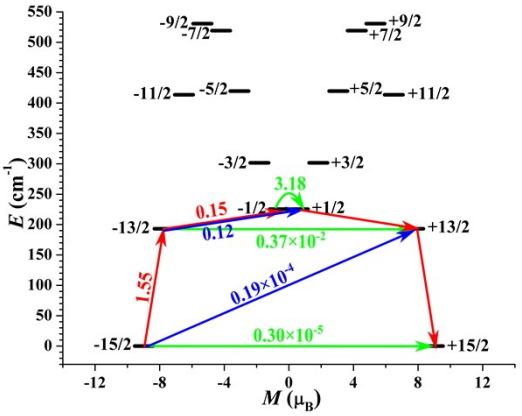

42.3°

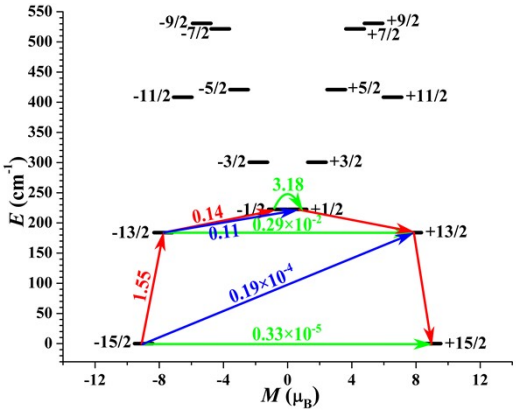

43.3°

44.3°

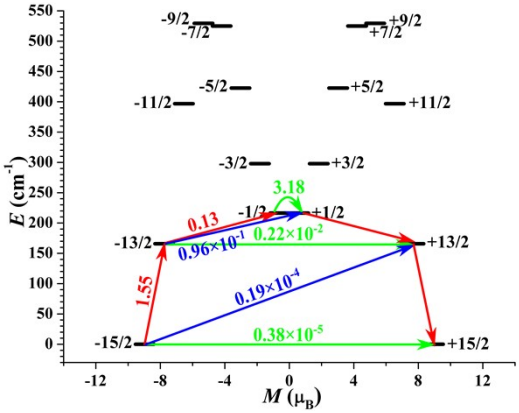

45.3°

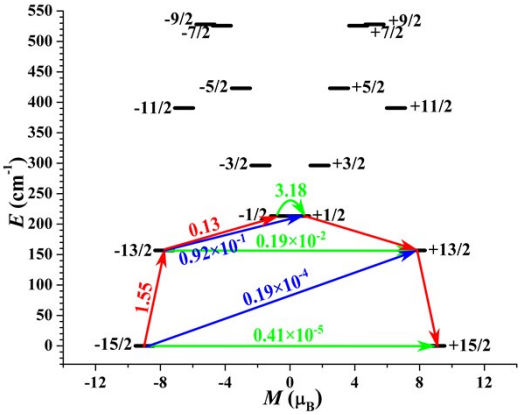

46.3°

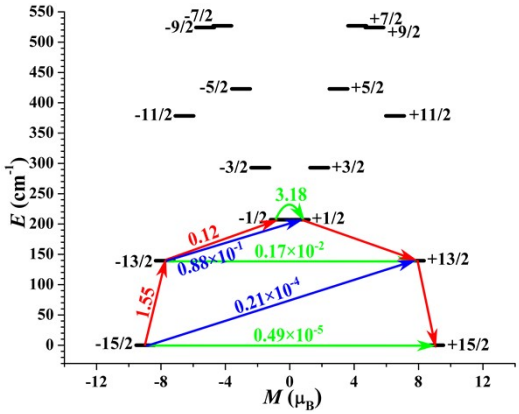

48.3°

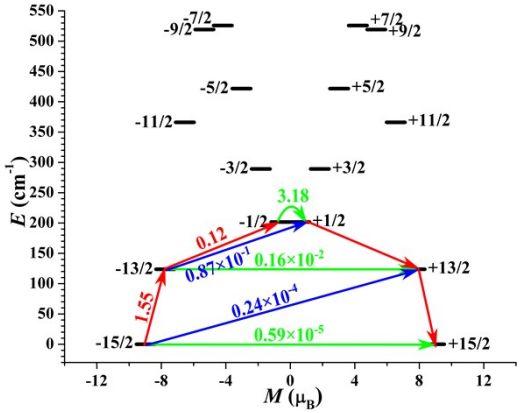

50.3°

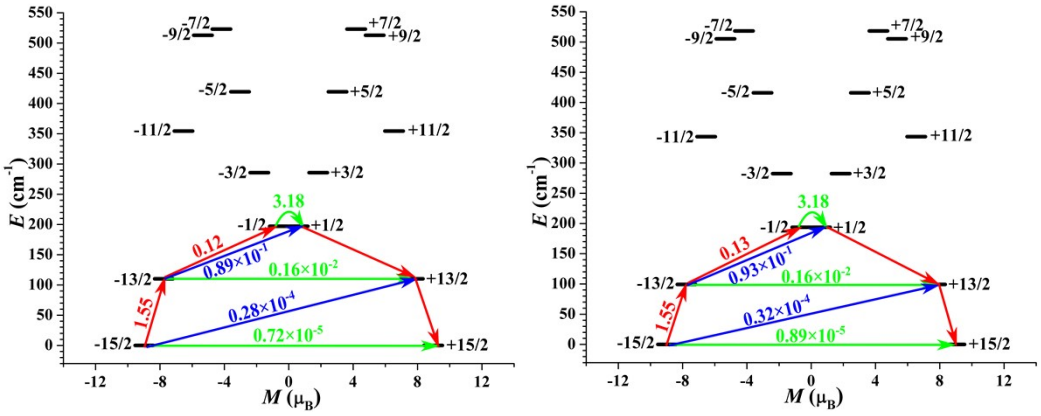

52.3° **54.3°**

Figure S5. Magnetization blocking barriers for **6** with different included θ angle (changing θ on one side of COT ligands) fixing the Er-C bond lengths. The thick black lines represent the KDs as a function of their magnetic moments along the magnetic axes. The green lines correspond to diagonal quantum tunneling of magnetization (QTM); the blue lines represent Orbach relaxation process. The path shown by the red arrows represents the most possibly path for magnetic relaxation in the corresponding compounds. The numbers at each arrow stand for the mean absolute value of the corresponding matrix element of transition magnetic moment.

Table S9. Average C-C bond lengths (Å) of one COT ligand with different θ angle.

θ	36.3°	38.3°	40.3°	42.3°	44.3°	46.3°	48.3°	50.3°	52.3°	54.3°
C-C	1.186	1.242	1.296	1.349	1.400	1.449	1.496	1.542	1.586	1.627

Table S10. Calculated crystal-field parameters B (k, q) and the corresponding weights for **6** with different included θ angle (changing the θ angles on one side of COT) keeping the Er-C bond lengths unchanged.

36.3°				**38.3°**				**40.3°**			
k	q	B (k, q)	Weight (%)	k	q	B (k, q)	Weight (%)	k	q	B (k, q)	Weight (%)
4	0	-0.13×10^{-1}	44.80	4	0	-0.13×10^{-1}	43.41	4	0	-0.13×10^{-1}	41.87
2	0	-0.15×10^{1}	29.15	2	0	-0.16×10^{1}	29.21	2	0	-0.16×10^{1}	29.26
6	0	0.41×10^{-4}	13.49	6	0	0.47×10^{-4}	14.94	6	0	0.53×10^{-4}	16.47
2	2	0.12	2.24	2	2	0.11	2.13	2	2	0.11	2.02
42.3°				**43.3°**				**44.3°**			
k	q	B (k, q)	Weight (%)	k	q	B (k, q)	Weight (%)	k	q	B (k, q)	Weight (%)
4	0	-0.13×10^{-1}	40.31	4	0	-0.12×10^{-1}	39.51	4	0	-0.12×10^{-1}	38.68
2	0	-0.17×10^{1}	29.34	2	0	-0.17×10^{1}	29.35	2	0	-0.17×10^{1}	29.32
6	0	0.60×10^{-4}	18.01	6	0	0.63×10^{-4}	18.75	6	0	0.66×10^{-4}	19.43
2	2	0.10	1.83	2	2	0.10	1.79	2	2	0.98×10^{-1}	1.68
45.3°				**46.3°**				**48.3°**			

k	q	B (k, q)	Weight (%)	k	q	B (k, q)	Weight (%)	k	q	B (k, q)	Weight (%)
4	0	-0.12×10^{-1}	37.81	4	0	-0.12×10^{-1}	36.96	4	0	-0.12×10^{-1}	35.47
2	0	-0.17×10^{1}	29.24	2	0	-0.17×10^{1}	29.16	2	0	-0.18×10^{1}	29.10
6	0	0.69×10^{-4}	20.05	6	0	0.72×10^{-4}	20.63	6	0	0.78×10^{-4}	21.70
2	–2	–0.10	1.72	2	–2	–0.11	1.79	2	–2	–0.12	1.95
50.3°				**52.3°**				**54.3°**			
k	q	B (k, q)	Weight (%)	k	q	B (k, q)	Weight (%)	k	q	B (k, q)	Weight (%)
4	0	-0.12×10^{-1}	34.42	4	0	-0.11×10^{-1}	33.41	4	0	-0.11×10^{-1}	32.60
2	0	-0.18×10^{1}	29.31	2	0	-0.18×10^{1}	29.47	2	0	-0.18×10^{1}	29.73
6	0	0.82×10^{-4}	22.77	6	0	0.85×10^{-4}	23.55	6	0	0.87×10^{-4}	24.14
2	–2	–0.13	2.12	2	–2	–0.14	2.20	2	–2	–0.14	2.20

Table S11. Calculated energy levels (cm^{-1}), $\boldsymbol{g}$ (g_x, g_y, g_z) tensors and predominant m_J values of the lowest eight KDs for **6** with different θ angles (changing the θ angles on the two sides of COT ligands simultaneously) fixing the Er-C bond lengths using CASSCF/RASSI-SO with OpenMolcas.

θ / KDs	**36.3°**			**38.3°**			**40.3°**		
	E	$\boldsymbol{g}$	m_J	E	$\boldsymbol{g}$	m_J	E	$\boldsymbol{g}$	m_J
1	0.0	0.000 0.000 17.953	±15/2	0.0	0.000 0.000 17.952	±15/2	0.0	0.000 0.000 17.950	±15/2
2	242.6	10.942 8.133 1.191	±1/2	240.9	10.668 8.422 1.206	±1/2	236.9	10.332 8.564 1.371	±1/2
3	294.7	0.981 1.169 6.532	±5/2	273.1	0.008 0.010 15.476	±13/2	244.0	0.098 0.118 15.346	±13/2
4	297.9	0.303 0.359 12.586	±13/2	300.0	1.018 1.212 3.660	±3/2	302.9	0.802 0.967 3.642	±3/2
5	381.9	0.057 0.339 6.037	±3/2	394.8	0.128 0.349 6.037	±5/2	406.9	0.194 0.374 6.043	±5/2
6	462.9	0.079 0.088 11.465	±11/2	455.8	0.014 0.015 12.995	±11/2	442.2	0.010 0.013 13.075	±11/2
7	472.1	0.105 0.126 10.103	±7/2	486.2	0.194 0.251 8.542	±7/2	501.6	0.213 0.323 8.452	±7/2
8	512.2	0.015 0.016 10.805	±9/2	520.9	0.026 0.029 10.778	±9/2	527.5	0.048 0.057 10.764	±9/2

θ / KDs	**42.3°**			**43.3°**			**44.3°**		
	E	$\boldsymbol{g}$	m_J	E	$\boldsymbol{g}$	m_J	E	$\boldsymbol{g}$	m_J
1	0.0	0.000 0.000 17.948	±15/2	0.0	0.000 0.000 17.948	±15/2	0.0	0.000 0.000 17.947	±15/2
2	208.4	0.014 0.015 15.491	±13/2	193.0	0.011 0.012 15.516	±13/2	175.0	0.007 0.008 15.523	±13/2
3	229.5	9.975 9.119 1.232	±1/2	225.1	10.160 8.932 1.230	±1/2	219.4	10.094 9.007 1.227	±1/2
4	303.0	0.311 0.561 3.673	±3/2	301.5	0.550 0.683 3.649	±3/2	299.3	0.482 0.609 3.652	±3/2
5	416.8	0.121 0.361 6.134	±5/2	413.8	0.027 0.048 12.994	±5/2	402.7	0.008 0.012 13.083	±11/2
6	423.3	0.000 0.015 13.001	±11/2	419.7	0.228 0.382 6.133	±11/2	422.0	0.289 0.432 6.058	±5/2
7	514.5	0.179 0.266 8.553	±7/2	519.4	0.130 0.520 8.460	±7/2	523.4	0.046 0.706 8.545	±7/2
8	530.7	0.024 0.052 10.888	±9/2	531.0	0.170 0.208 10.769	±9/2	530.2	0.330 0.405 10.818	±9/2
θ / KDs	**45.3°**			**46.3°**			**48.3°**		
	E	$\boldsymbol{g}$	m_J	E	$\boldsymbol{g}$	m_J	E	$\boldsymbol{g}$	m_J
1	0.0	0.000 0.000 17.946	±15/2	0.0	0.000 0.000 17.945	±15/2	0.0	0.000 0.000 17.943	±15/2
2	156.6	0.006 0.006 15.528	±13/2	138.1	0.005 0.005 15.531	±13/2	101.4	0.004 0.005 15.535	±13/2
3	212.9	10.033 9.072 1.227	±1/2	205.6	9.978 9.129 1.228	±1/2	188.7	9.886 9.222 1.230	±1/2
4	296.1	0.421 0.544 3.655	±3/2	292.0	0.368 0.486 3.658	±3/2	281.0	0.278 0.392 3.664	±3/2
5	390.7	0.005 0.007 13.087	±5/2	378.2	0.003 0.005 13.086	±5/2	351.7	0.001 0.005 13.080	±5/2
6	423.2	0.323	±11/2	423.3	0.354	±11/2	420.1	0.414	±11/2

		0.461 6.057			0.489 6.059			0.548 6.065	
7	526.1	0.765 1.508 9.577	±7/2	525.1	0.979 1.168 11.007	±9/2	516.3	0.319 0.416 10.699	±9/2
8	528.4	1.078 1.228 11.423	±9/2	528.1	0.549 1.467 9.014	±7/2	527.6	0.176 0.882 8.413	±7/2
θ / KDs	**50.3°**			**52.3°**			**54.3°**		
	E	***g***	m_J	*E*	***g***	m_J	*E*	***g***	m_J
1	0.0	0.000 0.000 17.940	±15/2	0.0	0.000 0.000 17.938	±15/2	0.0	0.001 0.002 17.655	±15/2
2	65.8	0.004 0.005 15.539	±13/2	32.2	0.005 0.005 15.546	±13/2	2.5	0.003 0.004 16.918	±13/2
3	169.0	9.812 9.293 1.232	±1/2	146.9	9.753 9.346 1.235	±1/2	123.2	9.704 9.384 1.242	±1/2
4	266.5	0.205 0.319 3.669	±3/2	248.6	0.149 0.265 3.676	±3/2	228.5	0.105 0.224 3.683	±3/2
5	323.7	0.000 0.006 13.072	±11/2	295.0	0.000 0.008 13.061	±11/2	266.9	0.000 0.011 13.044	±11/2
6	412.3	0.473 0.613 6.072	±5/2	400.1	0.534 0.683 6.078	±5/2	384.4	0.595 0.755 6.083	±5/2
7	503.3	0.235 0.315 10.674	±9/2	486.8	0.212 0.290 10.657	±9/2	467.9	0.210 0.291 10.642	±9/2
8	522.2	0.326 0.842 8.383	±7/2	512.0	0.419 0.879 8.370	±7/2	498.0	0.494 0.943 8.361	±7/2

Table S12. Wave functions with definite projection of the total moment $|m_J>$ for the lowest two or three KDs of $[Er(COT)_2]^-$ with different included θ angle (change the θ angles on the two sides of COT ligands simultaneously) keeping the Er-C bond lengths fixed.

θ	E/cm^{-1}	wave functions
36.3°	0.0	100%|±15/2>
	242.6	99.2%|±1/2>
38.3°	0.0	100%|±15/2>
	241.0	99.5%|±1/2>
40.3°	0.0	99.9%|±15/2>

	236.9	98.4%|±1/2>
42.3°	0.0	99.9%|±15/2>
	208.4	99.7%|±13/2>
	229.5	99.5%|±1/2>
43.3°	0.0	100%|±15/2>
	193.0	99.8%|±13/2>
	225.1	99.7%|±1/2>
44.3°	0.0	100%|±15/2>
	175.0	99.9%|±13/2>
	219.4	99.7%|±1/2>
45.3°	0.0	100%|±15/2>
	156.6	99.9%|±13/2>
	212.9	99.8%|±1/2>
46.3°	0.0	100%|±15/2>
	138.1	99.9%|±13/2>
	205.6	99.8%|±1/2>
48.3°	0.0	100%|±15/2>
	101.4	99.8%|±13/2>
	188.7	99.8%|±1/2>
50.3°	0.0	100%|±15/2>
	65.8	99.8%|±13/2>
	169.0	99.6%|±1/2>
52.3°	0.0	100%|±15/2>
	32.2	99.6%|±13/2>
	146.9	99.1%|±1/2>
54.3°	0.0	94.8%|±15/2>
	2.5	68.3%|±13/2>+24.6%|±11/2>
	123.2	44.6%|±3/2>+40.1%|±1/2>+13.5%|±5/2>

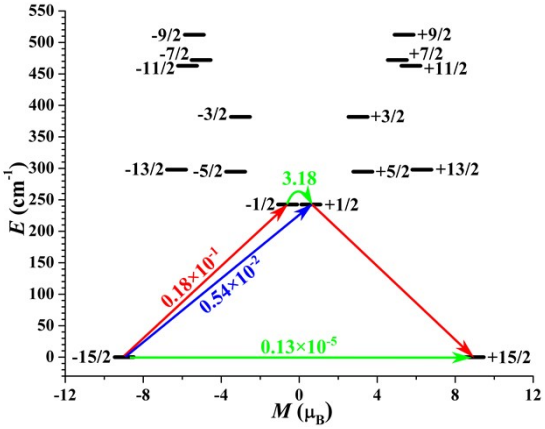

36.3°

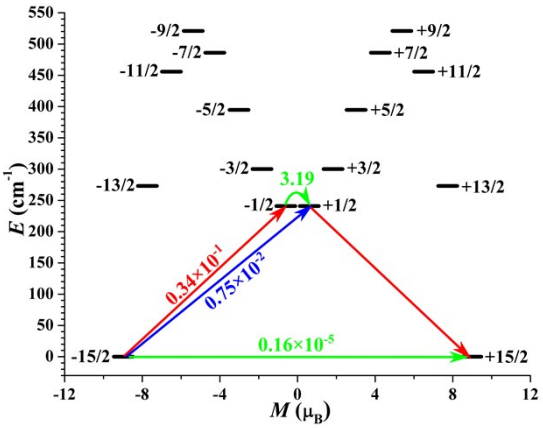

38.3°

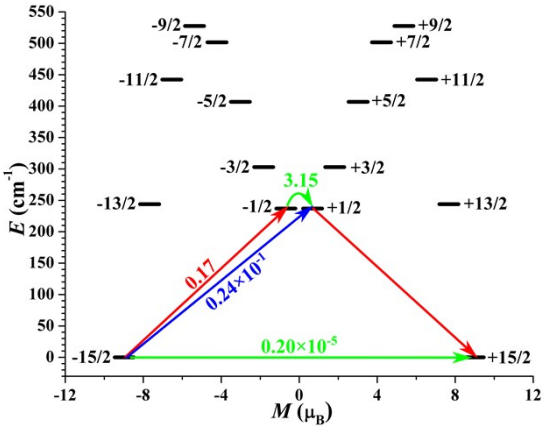

40.3°

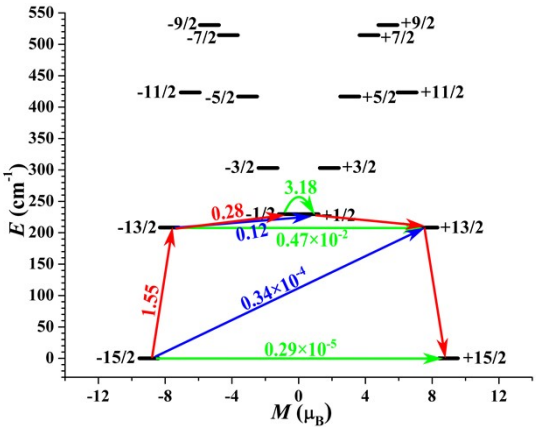

42.3°

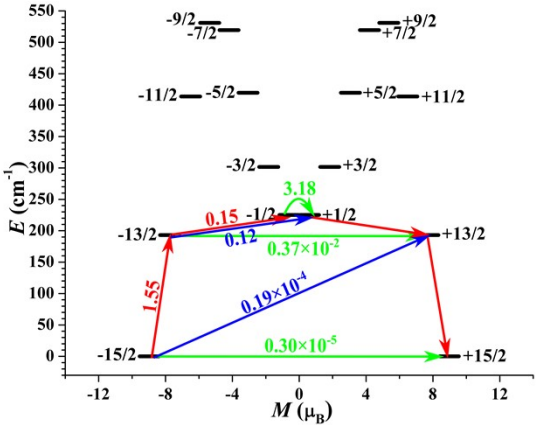

43.3°

44.3°

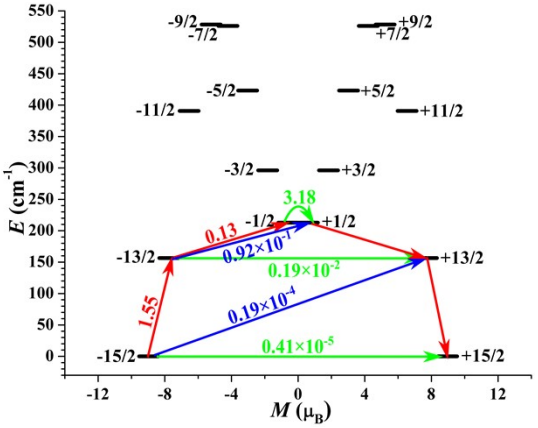

45.3°

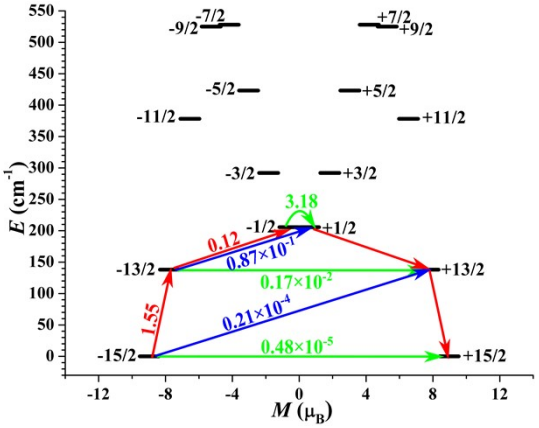

46.3°

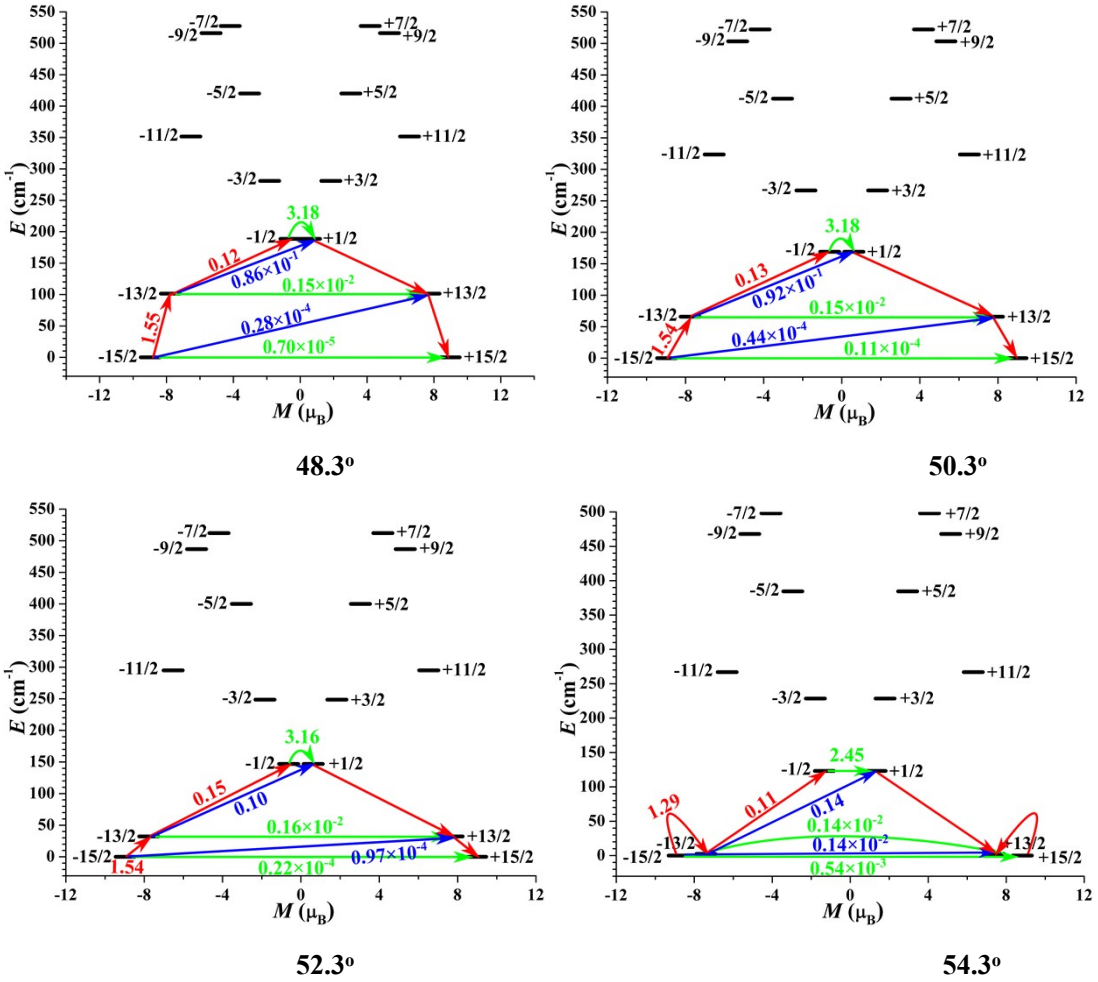

Figure S6. Magnetization blocking barriers for $[Er(COT)_2]^-$ with different included θ angle (change the θ angles on the two sides of COT ligands simultaneously) keeping the Er-C bond lengths fixed. The thick black lines represent the KDs as a function of their magnetic moments along the magnetic axes. The green lines correspond to diagonal quantum tunneling of magnetization (QTM); the blue lines represent Orbach relaxation process. The path shown by the red arrows represents the most possibly path for magnetic relaxation in the corresponding compounds. The numbers at each arrow stand for the mean absolute value of the corresponding matrix element of transition magnetic moment.

Table S13. The average C-C bond lengths (Å) of one COT ligands corresponding to different θ angles.

θ	**36.3°**	**38.3°**	**40.3°**	**42.3°**	**44.3°**	**46.3°**	**48.3°**	**50.3°**	**52.3°**	**54.3°**
C-C	1.186	1.242	1.296	1.352	1.400	1.449	1.496	1.542	1.586	1.627

Table S14. Calculated crystal-field parameters B (k, q) and the corresponding weights for $[Er(COT)_2]^-$ with different included θ angles (change the θ angles on the two sides of COT ligands simultaneously) keeping the Er-C bond lengths fixed.

36.3°				38.3°				40.3°			
k	*q*	*B* (*k*, *q*)	Weight (%)	*k*	*q*	*B* (*k*, *q*)	Weight (%)	*k*	*q*	*B* (*k*, *q*)	Weight (%)
4	0	-0.13×10^{-1}	52.21	4	0	-0.13×10^{-1}	48.94	4	0	-0.13×10^{-1}	45.49
2	0	-0.13×10^{1}	27.13	2	0	-0.14×10^{1}	27.99	2	0	-0.15×10^{1}	28.76
6	0	0.18×10^{-4}	6.57	6	0	0.29×10^{-4}	9.93	6	0	0.41×10^{-4}	13.33
2	2	0.12	2.63	2	2	0.12	2.45	2	2	0.12	2.25
42.3°				**43.3°**				**44.3°**			
k	*q*	*B* (*k*, *q*)	Weight (%)	*k*	*q*	*B* (*k*, *q*)	Weight (%)	*k*	*q*	*B* (*k*, *q*)	Weight (%)
4	0	-0.13×10^{-1}	41.22	4	0	-0.13×10^{-1}	40.31	4	0	-0.12×10^{-1}	38.68
2	0	-0.16×10^{1}	28.87	2	0	-0.17×10^{1}	29.30	2	0	-0.17×10^{1}	29.32
6	0	0.54×10^{-4}	16.49	6	0	0.60×10^{-4}	18.03	6	0	0.66×10^{-4}	19.43
6	–5	0.61×10^{-5}	1.86	2	2	0.11	1.88	2	2	0.98×10^{-1}	1.68
45.3°				**46.3°**				**48.3°**			
k	*q*	*B* (*k*, *q*)	Weight (%)	*k*	*q*	*B* (*k*, *q*)	Weight (%)	*k*	*q*	*B* (*k*, *q*)	Weight (%)
4	0	-0.12×10^{-1}	36.96	4	0	-0.12×10^{-1}	35.41	4	0	-0.11×10^{-1}	33.09
2	0	-0.17×10^{1}	29.14	2	0	-0.18×10^{1}	28.95	2	0	-0.18×10^{1}	28.85
6	0	0.72×10^{-4}	20.66	6	0	0.79×10^{-4}	21.84	6	0	0.90×10^{-4}	24.31
2	–2	–0.11	1.78	2	–2	–0.12	1.98	2	–2	–0.14	2.19
50.3°				**52.3°**				**54.3°**			
k	*q*	*B* (*k*, *q*)	Weight (%)	*k*	*q*	*B* (*k*, *q*)	Weight (%)	*k*	*q*	*B* (*k*, *q*)	Weight (%)
4	0	-0.11×10^{-1}	30.26	4	0	-0.10×10^{-1}	28.03	6	–1	0.11×10^{-3}	12.78
2	0	-0.18×10^{1}	27.79	6	0	0.11×10^{-3}	27.23	2	0	-0.16×10^{1}	11.50
6	0	0.10×10^{-3}	25.84	2	0	-0.18×10^{1}	26.77	4	–1	-0.76×10^{-2}	9.73
6	1	0.80×10^{-5}	2.05	6	1	0.15×10^{-4}	3.87	4	0	-0.72×10^{-2}	9.30

Table S15. Calculated energy levels (cm^{-1}), $\boldsymbol{g}$ (g_x, g_y, g_z) tensors and predominant m_J values of the lowest eight KDs for $[Er(COT)_2]^-$ with different Er-C bond lengths (Å) keeping the included angles $\theta = 54.3^o$ using CASSCF/RASSI-SO with OpenMolcas.

Er-C KDs	**2.02 Å**			**2.12 Å**			**2.22 Å**		
	E	***g***	m_J	*E*	***g***	m_J	*E*	***g***	m_J

1	0.0	10.114 8.628 1.409	±1/2	0.0	10.120 8.788 1.351	±1/2	0.0	10.066 8.930 1.315	±1/2
2	705.2	0.703 0.768 4.138	±3/2	510.5	0.618 0.696 4.049	±3/2	347.4	0.127 0.154 12.789	±11/2
3	1269.2	0.007 0.008 15.482	±13/2	702.9	0.005 0.008 15.422	±13/2	377.1	0.387 0.460 6.571	±5/2
4	1944.1	0.608 0.701 6.715	±5/2	1176.8	0.002 0.002 17.780	±15/2	639.3	0.000 0.001 17.855	±15/2
5	2049.8	0.016 0.018 17.469	±15/2	1363.8	0.673 0.779 6.343	±5/2	964.4	0.731 0.836 6.176	±3/2
6	2329.8	0.004 0.023 12.756	±11/2	1521.5	0.011 0.029 12.839	±11/2	993.9	0.048 0.076 12.876	±13/2
7	3027.6	0.609 0.656 8.452	±7/2	2084.4	0.614 0.767 8.430	±7/2	1454.4	0.389 0.996 8.424	±7/2
8	3130.3	0.029 0.038 10.444	±9/2	2140.0	0.061 0.069 10.529	±9/2	1476.0	0.269 0.311 10.594	±9/2
Er-C KDs	**2.32 Å**			**2.42 Å**			**2.52 Å**		
	E	***g***	m_J	*E*	***g***	m_J	*E*	***g***	m_J
1	0.0	9.959 9.068 1.309	±1/2	0.0	7.951 7.468 4.127	±3/2	0.0	0.024 0.025 15.521	±13/2
2	139.4	0.007 0.013 15.439	±13/2	11.4	1.763 1.894 12.661	±11/2	32.9	0.001 0.001 17.924	±15/2
3	268.8	0.385 0.482 4.002	±3/2	93.4	0.001 0.001 17.905	±15/2	73.9	9.655 9.392 1.268	±1/2
4	303.2	0.005 0.007 17.729	±15/2	197.9	0.241 0.348 3.752	±1/2	217.0	0.071 0.184 3.702	±3/2
5	644.2	0.022 0.030 12.971	±11/2	411.8	0.005 0.013 13.018	±13/2	325.0	0.001 0.010 13.043	±11/2
6	688.6	0.623 0.758	±5/2	497.6	0.626 0.763	±5/2	432.6	0.613 0.758	±5/2

		6.137			6.101			6.080	
7	1024.1	3.209 3.672 10.373	±9/2	715.3	0.418 0.511 10.629	±9/2	570.4	0.263 0.337 10.650	±9/2
8	1026.1	2.577 3.626 8.975	±7/2	731.5	0.298 1.198 8.360	±7/2	595.6	0.444 1.007 8.362	±7/2
Er-C KDs	**2.62 Å**			**2.72 Å**			**2.82 Å**		
	E	***g***	m_J	*E*	***g***	m_J	*E*	***g***	m_J
1	0.0	0.001 0.002 17.655	±15/2	0.0	0.000 0.000 17.941	±15/2	0.0	0.000 0.000 17.946	±15/2
2	2.5	0.003 0.004 16.918	±13/2	22.3	0.002 0.002 15.551	±13/2	35.9	0.001 0.001 15.548	±13/2
3	123.2	9.704 9.384 1.242	±1/2	170.7	9.954 9.099 1.254	±1/2	197.3	10.000 8.494 1.527	±1/2
4	228.5	0.105 0.224 3.683	±3/2	241.4	0.058 0.096 12.805	±11/2	219.6	0.222 0.345 12.631	±11/2
5	266.9	0.000 0.011 13.044	±11/2	249.0	0.331 0.462 3.885	±3/2	256.0	0.702 0.843 3.635	±3/2
6	384.4	0.595 0.755 6.083	±5/2	361.6	0.575 0.761 6.144	±5/2	337.0	0.503 0.746 6.458	±5/2
7	467.9	0.210 0.291 10.642	±9/2	408.4	0.185 0.306 10.575	±9/2	359.9	0.137 0.411 10.254	±9/2
8	498.0	0.494 0.943 8.361	±7/2	440.8	0.528 0.938 8.358	±7/2	392.3	0.567 0.972 8.354	±7/2

Er-C KDs	**2.92 Å**		
	E	***g***	m_J
1	0.0	0.000 0.000 17.949	±15/2
2	44.1	0.001 0.001 15.549	±13/2
3	197.5	0.618	±11/2

		0.762 12.269	
4	212.6	9.890 7.667 1.862	±1/2
5	254.7	1.125 1.284 3.610	±3/2
6	309.8	0.222 0.450 8.183	±5/2
7	321.9	0.204 0.780 8.519	±9/2
8	350.8	0.626 1.062 8.347	±7/2

Table S16. Wave functions with definite projection of the total moment | m_J > for the lowest two or three KDs for model $[Er(COT)_2]^-$ with the different Er-C bond lengths (Å) keeping the include angles θ = 54.3°.

θ	E/cm^{-1}	wave functions
2.02 Å	0.0	99.7%|±1/2>
	705.2	99.6%|±3/2>
2.12 Å	0.0	99.7%|±1/2>
	510.5	99.0%|±3/2>
2.22 Å	0.0	99.8%|±1/2>
	347.4	76.6%|±13/2>+23.4%|±3/2>
2.32 Å	0.0	99.6%|±1/2>
	139.4	99.1%|±13/2>
2.42 Å	0.0	79.1%|±1/2>+19.9%|±13/2>
	11.4	79.1%|±13/2>+19.7%|±1/2>
2.52 Å	0.0	98.2%|±13/2>
	32.9	98.9%|±15/2>
	73.9	98.5%|±1/2>
2.62 Å	0.0	94.8%|±15/2>
	2.5	68.3%|±13/2>+24.6%|±11/2>
	123.2	44.6%|±3/2>+40.1%|±1/2>+13.5%|±5/2>
2.72 Å	0.0	100%|±15/2>
	22.3	99.7%|±13/2>
	170.7	98.7%|±1/2>
2.82 Å	0.0	100%|±15/2>
	35.9	99.9%|±13/2>

	197.3	95.7%|±1/2>
2.92 Å	0.0	100%|±15/2>
	44.1	99.9%|±13/2>
	197.5	92.7%|±11/2>

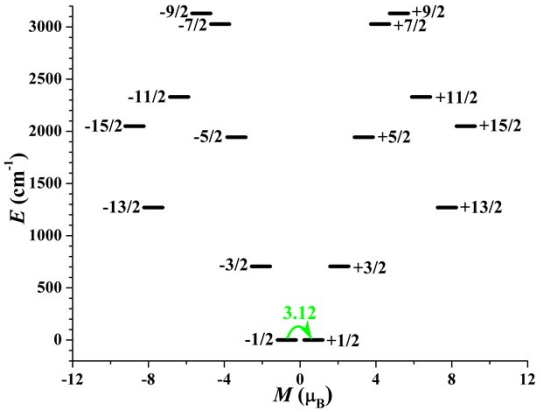

2.02 Å

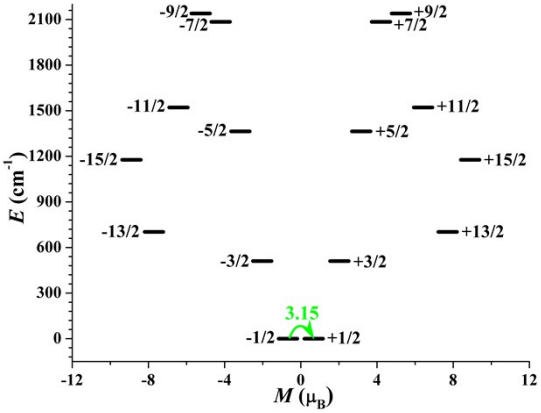

2.12 Å

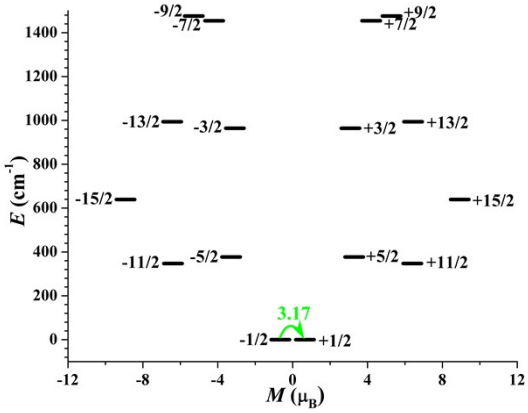

2.22 Å

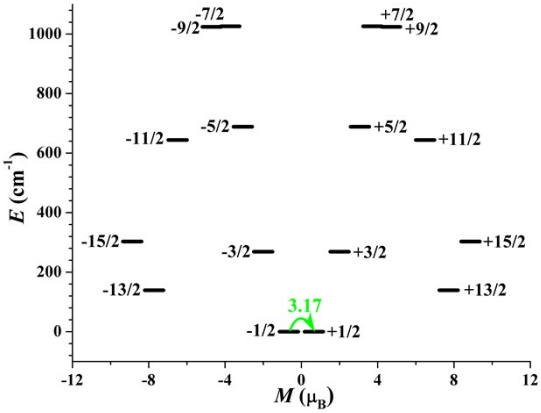

2.32 Å

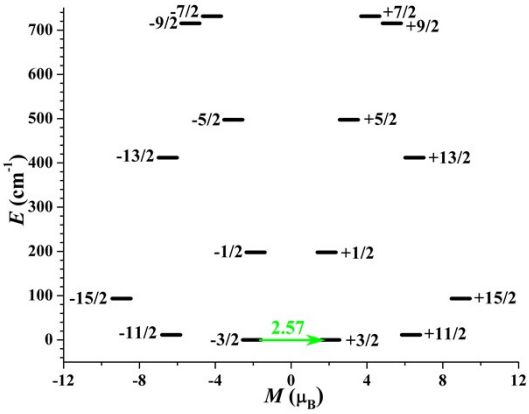

2.42 Å

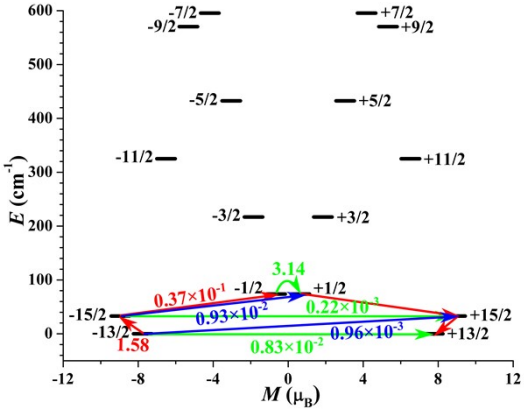

2.52 Å

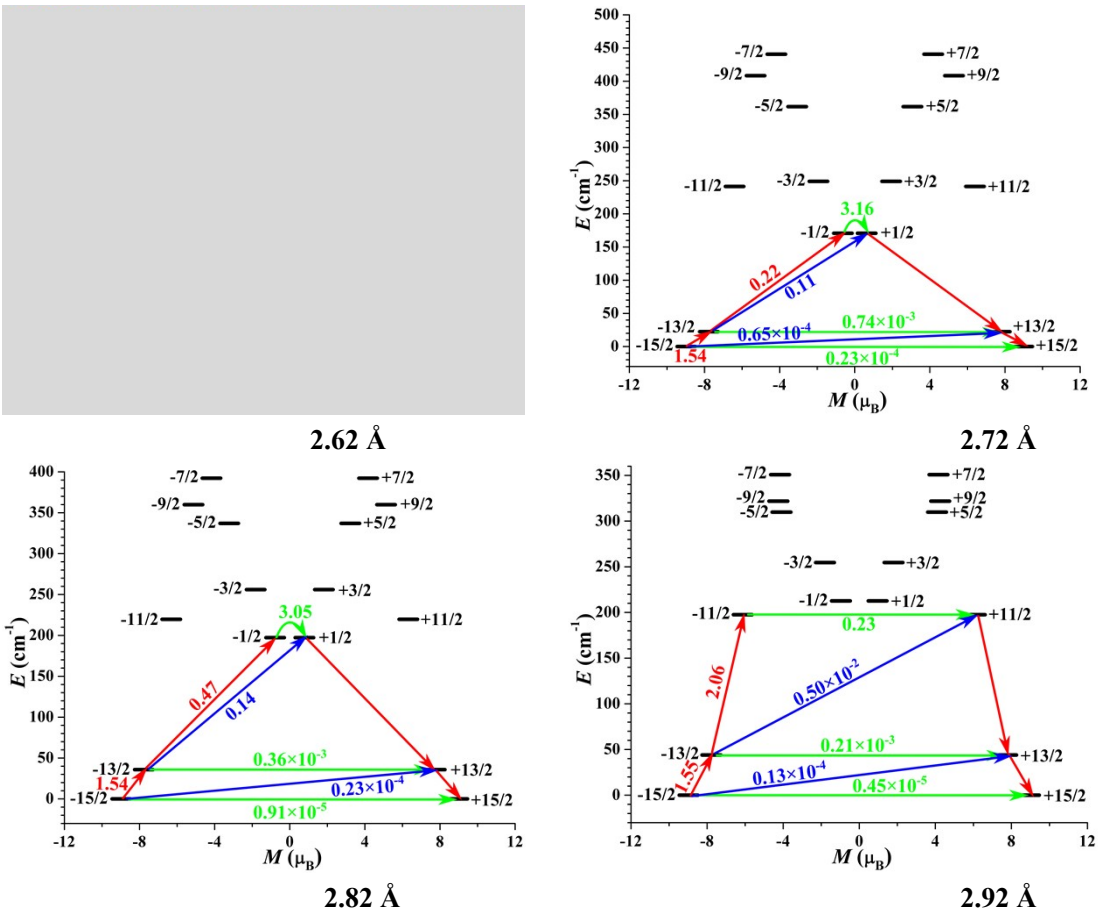

Figure S7. Magnetization blocking barriers for model $[Er(COT)_2]^-$ with the different Er-C bond lengths keeping the included angles θ = 54.3° unchanged. The thick black lines represent the KDs as a function of their magnetic moments along the magnetic axes. The green lines correspond to diagonal quantum tunneling of magnetization (QTM); the blue lines represent Orbach relaxation process. The path shown by the red arrows represents the most possibly path for magnetic relaxation in the corresponding compounds. The numbers at each arrow stand for the mean absolute value of the corresponding matrix element of transition magnetic moment.

Table S17. Average C-C bond lengths (Å) of two COT ligand rings with different Er-C bond lengths (Å).

Er-C	2.02	2.12	2.22	2.32	2.42	2.52	2.62	2.72	2.82	2.92
C-C	1.254	1.316	1.379	1.441	1.503	1.565	1.627	1.690	1.752	1.814

Table S18. Calculated crystal-field parameters B (k, q) and the corresponding weights for **6** with the different average Er-C bond lengths keeping θ = 54.3° unchanged.

2.02 Å				**2.12 Å**				**2.22 Å**			
k	q	B (k, q)	Weight (%)	k	q	B (k, q)	Weight (%)	k	q	$B(k, q)$	Weight (%)
6	0	0.77×10^{-3}	37.11	6	0	0.54×10^{-3}	40.17	6	0	0.39×10^{-3}	43.64
4	0	-0.61×10^{-1}	31.74	4	0	-0.44×10^{-1}	34.75	4	0	-0.32×10^{-1}	38.16

2	0	0.54×10^{1}	15.37	2	0	0.22×10^{1}	9.43	6	6	0.25×10^{-4}	2.78
6	6	0.53×10^{-4}	2.59	6	6	0.36×10^{-4}	2.70	6	2	-0.24×10^{-4}	2.71
2.32 Å				**2.42 Å**				**2.52 Å**			
k	*q*	*B* (*k*, *q*)	Weight (%)	*k*	*q*	*B* (*k*, *q*)	Weight (%)	*k*	*q*	*B* (*k*, *q*)	Weight (%)
6	0	0.28×10^{-3}	41.67	6	0	0.21×10^{-3}	33.37	6	0	0.15×10^{-3}	29.73
4	0	-0.23×10^{-1}	36.81	4	0	-0.17×10^{-1}	29.93	4	0	-0.13×10^{-1}	27.00
2	0	–0.74	6.44	2	0	-0.13×10^{1}	12.61	2	0	-0.16×10^{1}	18.58
6	2	-0.17×10^{-4}	2.54	6	1	-0.36×10^{-4}	5.87	6	–1	0.21×10^{-4}	4.08
2.62 Å				**2.72 Å**				**2.82 Å**			
k	*q*	*B* (*k*, *q*)	Weight (%)	*k*	*q*	*B* (*k*, *q*)	Weight (%)	*k*	*q*	*B* (*k*, *q*)	Weight (%)
6	–1	0.11×10^{-3}	12.78	2	0	-0.18×10^{1}	31.32	2	0	-0.18×10^{1}	37.65
2	0	-0.16×10^{1}	11.50	6	0	0.88×10^{-4}	25.98	6	0	0.68×10^{-4}	24.34
4	–1	-0.76×10^{-2}	9.73	4	0	-0.77×10^{-2}	24.21	4	0	-0.60×10^{-2}	23.01
4	0	-0.72×10^{-2}	9.30	6	1	-0.12×10^{-4}	3.40	2	2	–0.13	2.68
2.92 Å											
k	*q*	*B* (*k*, *q*)	Weight (%)								
2	0	-0.17×10^{1}	42.65								
6	0	0.52×10^{-4}	22.03								
4	0	-0.47×10^{-2}	21.21								
2	2	–0.11	2.83								

Table S19. Relevant structural parameters of models ***a***–***d***.

Model	Formula	φ[a] (degree)	Er–C[b] (Å)	Er–C[c] (Å)	C–C[d] (Å)	θ_X^e (degree)	θ_{COT}^e (degree)
a	$C_{13}H_{13}Er$	0.7	2.634	2.535	1.420	27.3	47.0
b	$C_{14}H_{14}Er$	0.9	2.780	2.501	1.415	30.4	47.9
c	$C_{16}H_{16}Er$	0.0	2.619	2.618	1.400	44.3	44.3
d	$C_{17}H_{17}Er$	0.7	2.854	2.582	1.418	46.4	46.0

[a] The dihedral angle between the planes of the upper and lower ligand rings. [b] The average Er–C(X) bond lengths for the ligand ring on the other side. [c] The average Er–C(COT) bond lengths. [d] The average C–C bond lengths of the two ligand rings. [e] θ_X represents the average included angle between the central axis perpendicular to the X ligand ring, and the vector connecting Er^{III} and the nearest X ligand atoms and θ_{COT} is the angle for the other side of COT ligand ring.

Table S20. Optimized coordinates of model ***a*** and ***b***.

a				***b***			
	x (Å)	*y* (Å)	*z* (Å)		*x* (Å)	*y* (Å)	*z* (Å)
C	–3.00526216	5.93811748	6.30770062	C	–3.00109177	5.94771260	6.28698059
C	–4.02417291	6.90988546	6.48647246	C	–4.02029985	6.92010838	6.46563000

C	–4.07355121	8.22727350	7.01272358	C	–4.06905743	8.23920288	6.98917147
C	–3.12418148	9.11870421	7.57732701	C	–3.11836263	9.13218376	7.55064735
C	–1.73252194	9.06171537	7.85038873	C	–1.72570769	9.07582471	7.82150392
C	–0.71355361	8.08981810	7.67149561	C	–0.70657926	8.10325315	7.64354769
C	–0.66418027	6.77249743	7.14542281	C	–0.65794935	6.78404580	7.12036432
C	–1.61348983	5.88100586	6.58085763	C	–1.60843547	5.89127201	6.55824247
Er	–2.70308340	6.85902766	8.64947598	Er	–2.68619951	6.89365878	8.57926140
C	–3.93442431	5.18303157	10.26693060	C	–4.28283886	5.31288593	10.21399283
C	–2.54498044	4.96274272	10.47205514	C	–4.42765212	6.61608091	10.72754603
C	–2.00071698	6.12670347	11.08056362	C	–3.31200206	7.29157662	11.25879680
C	–4.24900302	6.48313954	10.74865407	C	–2.05166252	6.66353579	11.27684841
C	–3.05387638	7.06643527	11.25158241	C	–1.90699121	5.36026081	10.76343118
H	–3.39655085	4.98743989	5.93988845	C	–3.02251126	4.68478256	10.23184653
H	–5.01320794	6.52951515	6.22321499	H	–3.38993645	5.00162400	5.90654622
H	–5.09143761	8.61978324	7.05750732	H	–5.00716347	6.54469917	6.18959261
H	–3.58513136	10.03430964	7.95337504	H	–5.08442332	8.63802163	7.02037746
H	–1.37680135	9.94410901	8.38614463	H	–3.57593450	10.05491014	7.91153016
H	0.23979471	8.40203288	8.10259638	H	–1.36618421	9.96556406	8.34128357
H	0.31784217	6.31142650	7.26887284	H	0.25089647	8.42228720	8.05886570
H	–1.18843403	4.89701965	6.37291628	H	0.32803459	6.32892459	7.22864426
H	–4.63662843	4.47554617	9.83019065	H	–1.18018625	4.91216093	6.33692285
H	–1.99685640	4.05703176	10.21987132	H	–5.14777215	4.78812631	9.80675087
H	–0.96300849	6.26802996	11.37656684	H	–5.40465349	7.10051348	10.71792133
H	–5.23438881	6.94515148	10.74597699	H	–3.42522407	8.29902015	11.66077791
H	–2.96386357	8.05313691	11.70188788	H	–1.18870565	7.18459060	11.69299514
				H	–0.93196254	4.87204704	10.78172012
				H	–2.91140386	3.67374585	9.83856068

Table S21. Calculated energy levels (cm^{-1}), ***g*** (g_x, g_y, g_z) tensors and predominant m_J values of the lowest eight KDs for models ***a***–***d*** using CASSCF/RASSI-SO with OpenMolcas.

KDs	***a***			***b***			***c***			***d***		
	E	***g***	m_J	*E*	***g***	m_J	*E*	***g***	m_J	*E*	***g***	m_J
1	0.0	0.000 0.000 17.948	±15/2	0.0	0.000 0.000 17.950	±15/2	0.0	0.000 0.000 17.947	±15/2	0.0	0.000 0.000 17.949	±15/2
2	197.8	0.064 5.284 11.056	±5/2	188.3	0.000 0.000 15.539	±13/2	175.0	0.007 0.008 15.523	±13/2	142.4	0.000 0.000 15.540	±13/2
3	201.1	8.363 6.323 1.680	±7/2	276.8	0.000 0.000 13.154	±11/2	219.4	10.094 9.007 1.227	±1/2	271.3	9.615 9.466 1.225	±1/2
4	206.1	3.416 2.815 1.297	±7/2	319.4	0.027 0.027 10.772	±9/2	299.3	0.482 0.609 3.652	±3/2	335.7	0.060 0.089 3.641	±3/2

5	211.2	8.693 8.218 0.497	±1/2	343.1	0.989 1.066 8.542	±7/2	402.7	0.008 0.012 13.083	±11/2	354.7	0.001 0.001 13.104	±11/2
6	217.1	0.130 0.466 11.147	±13/2	360.2	1.001 1.027 6.168	±5/2	422.0	0.289 0.432 6.058	±5/2	431.8	0.036 0.066 6.029	±5/2
7	226.3	0.089 0.127 8.610	±9/2	373.2	0.311 0.354 3.675	±3/2	523.4	0.046 0.706 8.545	±7/2	486.9	0.015 0.022 10.744	±9/2
8	249.2	0.903 0.954 13.062	±11/2	380.7	9.891 9.219 1.193	±1/2	530.2	0.330 0.405 10.818	±9/2	502.6	0.031 0.069 8.416	±7/2

Table S22. Wave functions with definite projection of the total moment | m_J > for the lowest two, three or five KDs for models ***a***–***d***.

θ	E/cm^{-1}	wave functions
a	0.0	100%|±15/2>
	197.8	71.3%|±5/2>+15.0%|±3/2>+11.5%|±7/2>
b	0.0	100%|±15/2>
	188.3	99.8%|±13/2>
	276.8	99.2%|±11/2>
	319.4	99.0%|±9/2>
	343.1	99.0%|±7/2>
c	0.0	100%|±15/2>
	175.0	99.9%|±13/2>
	219.4	99.7%|±1/2>
d	0.0	100%|±15/2>
	142.4	100%|±13/2>
	271.3	99.9|±1/2>

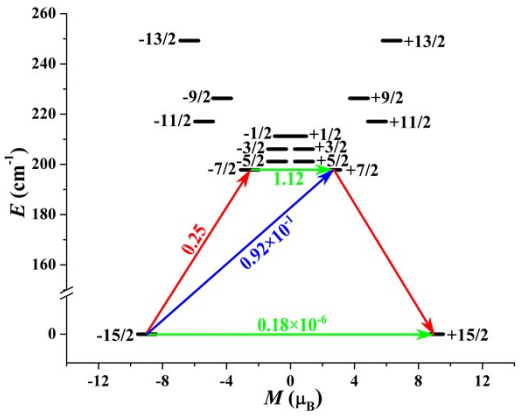

a

c

d

Figure S8. Magnetization blocking barriers for model ***a***, ***c*** and ***d***. The thick black lines represent the KDs as a function of their magnetic moments along the magnetic axes. The green lines correspond to diagonal quantum tunneling of magnetization (QTM); the blue lines represent Orbach relaxation process. The path shown by the red arrows represents the most possibly path for magnetic relaxation in the corresponding compounds. The numbers at each arrow stand for the mean absolute value of the corresponding matrix element of transition magnetic moment.

Table S23. Calculated crystal-field parameters $B(k, q)$ and the corresponding weights for models ***a***–***d***.

a				***b***				***c***			
k	q	$B(k, q)$	Weight (%)	k	q	$B(k, q)$	Weight (%)	k	q	$B(k,q)$	Weight (%)
4	0	-0.48×10^{-2}	34.90	2	0	-0.20×10^{1}	67.65	4	0	-0.12×10^{-1}	38.68
2	0	–0.79	31.67	4	0	-0.35×10^{-2}	20.89	2	0	-0.17×10^{1}	29.31
6	0	-0.30×10^{-4}	20.38	6	0	-0.11×10^{-4}	6.11	6	0	0.66×10^{-4}	19.43
6	–5	0.82×10^{-5}	5.59	6	1	-0.33×10^{-5}	1.88	2	2	0.98×10^{-1}	1.68

d			
k	q	$B(k, q)$	Weight (%)
2	0	-0.20×10^{1}	40.74
4	0	-0.96×10^{-2}	34.98
6	0	0.61×10^{-4}	20.77
6	–5	0.26×10^{-5}	0.90

References

S1. F. Aquilante, J. Autschbach, R. K. Carlson, L. F. Chibotaru, M. G. Delcey, L. De Vico, I. F. Galván, N. Ferré, L. M. Frutos, L. Gagliardi, M. Garavelli, A. Giussani, C. E. Hoyer, G. Li Manni, H. Lischka, D. Ma, P. Å. Malmqvist, T. Müller, A. Nenov, M. Olivucci, T. B. Pedersen, D. Peng, F. Plasser, B. Pritchard, M. Reiher, I. Rivalta, I. Schapiro, J. Segarra-Martí, M. Stenrup, D. G. Truhlar, L. Ungur, A. Valentini, S. Vancoillie, V. Veryazov, V. P. Vysotskiy, O. Weingart, F. Zapata and R. Lindh, *J. Comput. Chem.*, 2016, **37**, 506–541.

S2. F. Neese, ORCA–*an ab initio, density functional and semiempirical program package*, Version 5.0.1; Max-Planck institute for bioinorganic chemistry: Mülheim an der Ruhr, Germany, 2021.

S3. C. Angeli, R. Cimiraglia and J. P. Malrieu, *J. Chem. Phys.*, 2002, **117**, 9138–9153.

S4. C. Angeli, R. Cimiraglia, S. Evangelisti, T. Leininger and J. P. Malrieu, *J. Chem. Phys.*, 2001, **114**, 10252–10264.

S5. C. Angeli, R. Cimiraglia and J. P. Malrieu, *Chem. Phys. Lett.*, 2001, **350**, 297–305.

S6. C. Angeli and R. Cimiraglia, *Theor. Chem. Acc.*, 2002, **107**, 313–317.

S7. D. Aravena, F. Neese and D. A. Pantazis, *J. Chem. Theory Comput.*, 2016, **12**, 1148–1156.

S8. F. Weigend and R. Ahlrichs, *Phys. Chem. Chem. Phys.*, 2005, **7**, 3297–3305.

S9. M. Roemelt and F. Neese, *J. Phys. Chem. A*, 2013, **117**, 3069–3083.